

Development of algorithm to model dispersed gas-liquid flow using lattice Boltzmann method

Alankar Agarwal^{a,*}, B. Ravindra^a, Akshay Prakash^b

^a*Indian Institute of Technology Jodhpur, Jodhpur, Rajasthan, India-342037*

^b*Indian Institute of Technology Kharagpur, Kharagpur, West Bengal, India-721302*

Abstract

In this paper, we present the algorithm for the simulation of a single bubble rising in a stagnant liquid using Euler-Lagrangian (EL) approach. The continuous liquid phase is modeled using BGK approximation of lattice Boltzmann method (LBM), and a Lagrangian particle tracking (LPT) approach has been used to model the dispersed gas (bubble) phase. A two-way coupling scheme is implemented for the interface interaction between two phases. The simulation results are compared with the theoretical and experimental data reported in the literature and it was found that the presented modeling technique is in good agreement with the theoretical and experimental data for the relative and terminal velocity of a bubble. We also performed the grid independence test for the current model and the results show that the grid size does not affect the rationality of the results. The stability test has been done by finding the relative velocity of a bubble as a function of time for the different value of dimensionless relaxation frequency. The present study is relevant for understanding the bubble-fluid interaction module and helps to develop the accurate numerical model for bioreactor simulation.

Keywords: Computational Fluid Dynamics; Multiphase flow; Bubble-fluid interaction; Lattice Boltzmann method; Lagrangian particle tracking

*Corresponding author

Email address: agarwal.1@iitj.ac.in (Alankar Agarwal)

1. Introduction

Bubble column reactors are widely encountered in chemical, biological and pharmaceutical industry. The motion of dispersed air bubble in its process has been the focus of research for a long time [1]. In the past few decades, a number of experimental investigations [2, 3, 4] have been performed to understand the basic underlying physics and its hydrodynamics [5]. Based on the empirical relations obtained from experiments, researchers developed various numerical models or computational fluid dynamics (CFD) techniques for this multiphase problem. These models are categorized based on their treatment of dispersed (gas) phase into continuous (liquid) phase [6] as follows:

- **Euler-Euler (EE)** model also referred as two-fluid model, where both the dispersed (gas bubble) and continuous (liquid) phase are treated as interpenetrating continua, and interaction between the two phases are modeled using the phase interaction terms that appear in the conservation equations, describes the dynamics of the system [7],
- **Euler-Lagrangian (EL)** model, in which the liquid phase is modeled in eulerian cell, while the dispersed gas bubble is treated as Lagrangian marker. The motion of bubbles is governed by the Newton's law of motion. The Euler-Lagrangian approach requires closure relations for the forces between two-phases, which can be obtained from the experimental correlations or from simulations with higher level of details (e.g volume-of-fluid (VOF) or front-tracking (FT) method) [8].

This work is focused on the Eulerian-Lagrangian (EL) approach to simulate the dispersed gas-liquid flow problem. Although a version of this approach has already been reported in the literature, the present study uses the BGK scheme of lattice Boltzmann method (LBM) to model the continuous liquid phase in a Eulerian frame of reference and the motion of dispersed gas bubble is computed using Lagrangian particle tracking (LPT) approach. The two-way coupling for momentum transfer between the phases is achieved with the cheap-clipped

polynomial mapping function proposed by [9].

In recent decades, lattice Boltzmann Method (LBM) has emerged as a powerful numerical tool to simulate multiphase flows. The method based on the molecular kinetic theory shows numerous advantages over conventional computational fluid dynamics (CFD) method. The method has been proven to be an efficient algorithm for the simulation of complex boundary problems, and due to explicit nature, it is easily parallelizable [10]. The interested reader is referred to [11, 12, 13, 14] for more information about the various multiphase models of lattice Boltzmann method (LBM).

This paper is organized in the following manner: The methodology to simulate dispersed gas-liquid flow is reported in section 2, which describes the governing equations for bubble and liquid phase hydrodynamics in its subsequent subsection. In section 3, the test flow problem is described along with geometry and simulation parameters, the coupling between two phases and boundary-conditions. The results are discussed in section 4. Section 5 provides the summary of the work and concludes the paper.

2. Methodology

In this study, an air bubble is released in a 3D rectangular column tank filled with stagnant water. The transient, three-dimensional Euler-Lagrange model is used to simulate this multiphase problem. The model consists of two processes: the first process includes the bubble motion and the second part describes the liquid velocity fluctuations. The EL model requires constitutive equations to couple two processes through the forces acting between a bubble and liquid [15]. The interaction between the dispersed (gas) phase and continuous (liquid) phase can be modeled with the two-way coupling approach.

2.1. Bubble dynamics

The air bubble in a stagnant water tank is treated as a point-volume particle with constant mass [8], the motion of bubble is computed from the Newton's

second law of motion:

$$m_b(d\mathbf{u}_b/dt) = \sum \mathbf{F}_b \quad (1)$$

where \mathbf{u}_b , m_b , and \mathbf{F}_b are the velocity, mass and total force acting on the bubble respectively. The net force acting on bubble is composed of several external forces i.e. buoyancy force \mathbf{F}_B , stress gradient force \mathbf{F}_S , drag force \mathbf{F}_D , lift force \mathbf{F}_L and virtual mass force \mathbf{F}_{VM} gives:

$$\mathbf{F}_b = \mathbf{F}_B + \mathbf{F}_S + \mathbf{F}_{VM} + \mathbf{F}_D + \mathbf{F}_L \quad (2)$$

An expression to compute these forces is given in Table 1.

Table 1: Expression for interface forces acting on bubble [16], [8]

Force	Coefficient relation
$\mathbf{F}_B = (\rho_l - \rho_b)V_b g$	-
$\mathbf{F}_S = \rho_l V_b D_t \mathbf{u}_l$	-
$\mathbf{F}_{VM} = -C_A \rho_l V_b (D_t \mathbf{u}_b - D_t \mathbf{u}_l)$	$C_A = 0.5$
$\mathbf{F}_D = \frac{-1}{2} C_D \rho_l \pi r_b^2 \mathbf{u}_b - \mathbf{u}_l (\mathbf{u}_b - \mathbf{u}_l)$	$C_D = \max[\min\frac{24}{Re}(1 + 0.015Re^{0.687}, \frac{48}{Re}, \frac{8}{3} \frac{E_o}{E_o+4}]$
$\mathbf{F}_L = -C_L \rho_l V_b (\mathbf{u}_b - \mathbf{u}_l) \times \nabla \times \mathbf{u}_l$	$C_L = \begin{cases} \min[0.288 \tanh(0.121 Re, f(E_{od}))], & E_{od} < 4 \\ f(E_{od}), & 4 < E_{od} \leq 10 \\ -0.29, & E_{od} > 10 \end{cases}$
	$E_{od} = \frac{E_o}{E_o^{2/3}}, E = \frac{1}{1+0.163E_o^{0.757}}$
	$f(E_{od}) = 0.00105E_{od}^3 - 0.0159E_{od}^2 - 0.0204E_{od}$

where the Eotvos number, E_o and Reynolds number, Re can be calculated as follows [15]:

$$E_o = (\rho_l - \rho_b)gd_b/\sigma, \quad Re = \rho_l(\mathbf{u}_b - \mathbf{u}_l)/\mu_l \quad (3)$$

where, ρ_l , ρ_b , \mathbf{u}_b and \mathbf{u}_l represent the liquid density, air-bubble density, bubble velocity and liquid velocity respectively. Due to these forces acting on bubble, it start accelerating. The bubble velocity at next time step can be computed using the expression below:

$$\mathbf{u}_b^{n+1} = \mathbf{u}_b^n + \left[\left(\sum \mathbf{F}_b \right) / m_b \right] \Delta t_b \quad (4)$$

where, Δt_b is the time step for dispersed air bubble calculation.

2.2. Liquid phase hydrodynamics: LBGK model

The continuous fluid in this gas-liquid flow is discretized using nineteen velocity (D_3Q_{19}) lattice Bhatnagar-Gross and Krook (LBGK) model on cubic lattice. The model is also popularly known as single-relaxation time (SRT) model. The schematic representation of D_3Q_{19} lattice structure is shown in Fig.1.

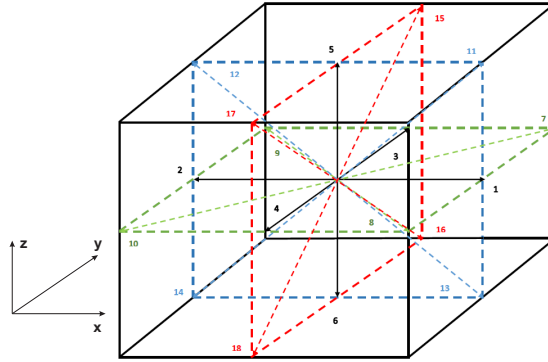


Fig. 1. Schematic representaion of D_3Q_{19} lattice structure

The lattice Boltzmann equation (LBE) with single-relaxation time (SRT) parameter without a forcing term can be written as [17]:

$$f_j(x + c_j \Delta t_l, t_l + \Delta t_l) = f_j(x, t_l) - (1/\tau)[f_j(x, t_l) - f_j^{eq}(x, t_l)] \quad (5)$$

where f is the probability density distribution function (PDDF). The equilibrium probability density distribution function can be computed as [18]:

$$f_j^{eq} = w_j \rho_l \left[1 + \frac{3}{e^2} (c_j \cdot \mathbf{u}_l) + \frac{9}{2e^4} (c_j \cdot \mathbf{u}_l)^2 - \frac{3}{2e^2} \mathbf{u}_l^2 \right] \quad (6)$$

For the D_3Q_{19} model the discrete velocity vectors c_j , and the corresponding weighted function w_j can be expressed as [19]:

$$c_j = \begin{cases} e(\pm 1, 0, 0), e(0, \pm 1, 0), e(0, 0, \pm 1), & j = 1, \dots, 6 \\ e(\pm 1, \pm 1, 0), e(\pm 1, 0, \pm 1), e(0, \pm 1, \pm 1), & j = 7, \dots, 18 \\ e(0, 0, 0), & j = 19 \end{cases} \quad (7)$$

$$w_j = \begin{cases} 1/18, & j = 1, \dots, 6 \\ 1/36, & j = 7, \dots, 18 \\ 1/3, & j = 19 \end{cases} \quad (8)$$

where the lattice speed $e = \frac{\Delta x}{\Delta t_l}$, and Δx and Δt_l are the respective lattice size and the time step for the calculation of continuous liquid phase. The dimensionless relaxation time parameter τ is related to the kinematic viscosity that fixes the rate of approach to equilibrium given by [20]:

$$\nu = \left((2\tau - 1)/6 \right) * \left((\Delta x)^2 / \Delta t_l \right), \quad \tau = 1/\omega \quad (9)$$

where, ω is the dimensionless relaxation frequency.

The macroscopic variables such as density per node and momentum density are computed from the real-valued PDDF by [18]:

$$\rho_l = \sum_j f_j = \sum_j f_j^{eq}, \quad \rho_l \mathbf{u}_l = \sum_j c_j f_j = \sum_j c_j f_j^{eq} \quad (10)$$

This density and momentum density satisfy the traditional pressure-based solver (i.e. Navier-Stokes solver) for incompressible flow explained by using the Chapman-Enskog expansion [21].

When an external force is applied in the computational cell, the LBE equation can be defined as [22]:

$$f_j(x + c_j \Delta t_l, t_l + \Delta t_l) = f_j(x, t_l) - (1/\tau)[f_j(x, t_l) - f_j^{eq}(x, t_l)] + F_j(x, t_l) \Delta t_l \quad (11)$$

The corresponding discrete force distribution function can be given by the following relation [23]:

$$F_j(x, t_l) = (1 - (1/2\tau)) w_j \left[3 \left\{ (c_j - \mathbf{u}_l(x, t_l)) / e^2 \right\} + 9 \left\{ (c_j \mathbf{u}_l) / e^4 \right\} c_j \right] \cdot \mathbf{F}(x, t_l) \quad (12)$$

where \mathbf{F} is the external force on the liquid phase.

The numerical technique to solve the LBE equation with an external force term is as follows [17]:

First-forcing step:

$$\rho_l(x, t_l)\mathbf{u}_1(x, t_l) = \sum_{j=1}^9 c_j f_j(x, t_l) + (\Delta t_l/2)\mathbf{F}(x, t_l) \quad (13)$$

Collision step:

$$f'_j(x, t_l) = f_j(x, t_l) - (1/\tau)[f_j(x, t_l) - f_j^{eq}(x, t_l)] \quad (14)$$

Second-forcing step:

$$f''_j(x, t_l) = f'_j(x, t_l) + \Delta t_l F_j(x, t_l) \quad (15)$$

Streaming step:

$$f_j(x + c_j \Delta t_l, t_l + \Delta t_l) = f''_j(x, t_l) \quad (16)$$

3. Numerical Modelling

3.1. Geometry and simulation parameters

In this study, a three-dimensional (3D) rectangular bubble column with dimension $0.15 \text{ m} \times 0.15 \text{ m} \times 1 \text{ m}$ is considered for the simulation. The water is filled up to the height of 0.45 m . Initially, a spherical air-bubble of diameter 4 mm is released in water. It was assumed that the bubble remains spherical throughout the simulation [8].

The aspect ratio (a_r) between the cell size Δx and bubble diameter d_b was chosen to be 1.25 as given by [24]:

$$a_r = \Delta x/d_b = 1.25 \quad (17)$$

The conversion of the physical unit to lattice unit is shown in Appendix A. Simulation conditions for the rising of a single bubble in a stagnant liquid are given in Table 2. The physical properties for the continuous (water) and dispersed (air-bubble) phase used in this simulation are given in Table 3.

Table 2: Simulation conditions for bubble of 4 mm diameter rising in a quiescent water tank

Physical domain	0.15 m \times 0.15 m \times 0.45 m
Computational domain	30 \times 30 \times 90
Liquid time step	0.0001 sec
Bubble time step	0.00001 sec
Simulation time	2.0000 sec

Table 3: Physical properties of dispersed air bubble and continuous liquid phase [9]

Phase	Property	Unit	Value
Dispersed phase (air-bubble)	Density (ρ_b)	kg/m^3	1.0
	Diameter (d_b)	m	0.004
	Viscosity (μ_b)	$kg/m - s$	1.8×10^{-5}
Continuous phase (water)	Density (ρ_l)	kg/m^3	1000
	Viscosity (μ_l)	$kg/m - s$	0.001
	Surface tension (σ)	N/m	0.073

3.2. Interphase coupling

A two-way coupling between the continuous and dispersed phase is done by the cheap clipped fourth-order polynomial mapping function. The mapping function was introduced by [9], which translates the influence of Eulerian quantities on Lagrangian position and vice-versa. The mapping function should satisfy the following criteria given below [25]:

- It should be a smooth function, i.e. the first derivation should be continuous.
- It should have an absolute maximum around the position where the variable is transferred.
- For practical reasons, it should have a finite domain. At the boundaries of the domain, the function should be zero.

- The integral of the function over the entire domain should equal unity.

The mapping function for this two-phase coupling is given as [9, 15]:

$$Z(x_l - x_b) = \begin{cases} \frac{15}{16} \left[\frac{(x_l - x_b)}{n^5} - 2 \frac{(x_l - x_b)}{n^3} + \frac{1}{n} \right], & -n \leq ((x_l - x_b)) \leq n \\ 0, & otherwise \end{cases} \quad (18)$$

where x_b is the position vector of gas bubble and $n = 1.5d_b$ is the width of the mapping window. For the three-dimensional (3D) domain, the influence of eulerian quantities (i.e. *velocity*, *vorticity*) on bubble position is evaluated using the given relation [9]:

$$\int_{\Omega_j} Z d\Omega = \int_{\Omega_{j,y}} \int_{\Omega_{j,x}} Z(x_l - x_b) Z(y_l - y_b) Z(z_l - z_b) dx dy dz \quad (19)$$

$$\Psi = \sum_j \sigma(j) \int_{\Omega_j} Z d\Omega \quad (20)$$

where,

- Ψ defines the influenced eulerian quantities at bubble position
- x_l, y_l, z_l are the position coordinates of liquid computational cell j
- x_b, y_b, z_b are the bubble centroids
- σ be the corresponding eulerian quantity

Similarly, the influence of lagrangian quantity on the liquid computational cell j is calculated using the formula:

$$\Phi(j) = \psi_b \int_{\Omega_j} Z d\Omega \quad (21)$$

where, ψ_b is the reaction of the momentum transfer exerted on the bubble, i.e. $\psi_b = -\sum \mathbf{F}$

Algorithm 1 LBGK-LPT approach to model dispersed gas-liquid flows

Input: Physical properties of continuous (liquid) and dispersed (gas) phase

Output: out

Initialisation : Calculating PDDF in velocity space

$$f_j = w_j \rho_l [1 + \frac{3}{e^2} (c_j \cdot \mathbf{u}_1) + \frac{9}{2e^4} (c_j \cdot \mathbf{u}_1)^2 - \frac{3}{2e^2} \mathbf{u}_1^2]$$

LOOP Process

1: **for** $i = 1$ to t **do**

2: Tracked bubble position in the domain and select the nearest eulerian node which interact with bubble.

3: **Forward coupling:** mapping of eulerian (liquid) quantities on lagrangian (air-bubble) position, i.e. *velocity, vorticity*: $\Psi = \sum_j \sigma(j) \int_{\Omega_j} Z d\Omega$

4: **Net force on bubble:** calculate total force acting on bubble i.e. *buoyancy, stress gradient, drag, lift* and *virtual mass* using:

$$\mathbf{F}_b = \mathbf{F}_G + \mathbf{F}_S + \mathbf{F}_D + \mathbf{F}_L + \mathbf{F}_{VM}$$

5: **Update bubble velocity and position:** The velocity and position of bubble can be updated using:

$$\mathbf{u}_b^{n+1} = \mathbf{u}_b^n + \frac{\mathbf{F}_b}{m_b} \Delta t_b, x_b^{n+1} = x_b^n + S$$

6: **Backward coupling:** Mapped the reaction force calculated from the updated lagrangian (i.e. bubble) velocity on the eulerian (liquid) cell using:

$$\psi_b = -(\mathbf{F}_D + \mathbf{F}_L) = -\mathbf{F}$$

$$\Phi(j) = \psi_b \int_{\Omega_j} Z d\Omega$$

7: **Discrete force distribution function:** The reaction force that mapped on eulerian node from lagrangian frame is defined in the discrete form as:

$$F_j(x, t) = (1 - \frac{1}{2\tau}) w_j [3 \frac{c_j - \mathbf{u}_1(x, t)}{e^2} + 9 \frac{c_j \mathbf{u}_1(x, t)}{e^4} c_j] * \Phi(j)$$

8: **Equilibrium, PDDF:** The equilibrium, PDDF can be calculated as:

$$f_j^{eq} = w_j \rho_l [1 + \frac{3}{e^2} (c_j \cdot \mathbf{u}_1) + \frac{9}{2e^4} (c_j \cdot \mathbf{u}_1)^2 - \frac{3}{2e^2} \mathbf{u}_1^2]$$

9: perform first forcing step, collision step, second forcing step and streaming step on eulerian computational cell given in section 2.2, provide boundary-conditions and update macroscopic properties for liquid i.e. *velocity, momentum density*

10: **if** bubble reaches top layer of fluid **then**

11: stop 10

12: **end if**

13: **end for**

14: **return** 2

3.3. Boundary-conditions

A no-slip boundary condition based on non-equilibrium half-way bounce-back condition given by [26] are applied to every side of the computational domain except for the top boundary of the domain where a free-slip boundary condition is applied [8]. Algorithm 1 explains the detailed procedure for simulating the dispersed gas-liquid flows using LBGK-LPT model.

4. Results and Discussion

4.1. Validation test

In this section, simulation results of a single bubble rising in a 3D rectangular liquid column using LBGK-LPT approach are compared with theoretical and available experimental data in the literature. The relative velocity of bubble motion at different time instant can be calculated theoretically using the expression below:

$$d\mathbf{v}_r/dt = (\mathbf{F}_B + \mathbf{F}_D)/m_b \quad (22)$$

where \mathbf{v}_r be the velocity of bubble motion relative to the velocity of the liquid phase.

The terminal velocity of the bubble is calculated theoretically using the force balance equation. A bubble rising in a quiescent liquid attains a constant velocity when the net gravity force will be equal to the drag force on the bubble. The force balance equation can be defined as:

$$(\rho_l - \rho_b)V_b g = (1/2) * (C_D v_T^2 \pi r_b^2) \quad (23)$$

where, v_T represent the terminal velocity of bubble. Solving Eq.(23) gives an expression for terminal velocity:

$$v_T = \sqrt{\left\{ (\rho_l - \rho_b)V_b g \right\} / \left\{ (1/2)(C_D \pi r_b^2) \right\}} \quad (24)$$

The results are also validated for terminal velocity at a different case of bubble diameter with Mendelson equation given by [27]. The equation was given as

[28]:

$$v_{T_M} = \sqrt{\left\{2\sigma/(\rho_l d_b)\right\} + \left\{gd_b/2\right\}} \quad (25)$$

The comparison of simulated, theoretical and experimental terminal velocity

Table 4: Comparison of predicted, theoretical and experimental terminal velocity at a different case of bubble diameter [28], [2]

Bubble diameter (mm)	Simulation (LBGK-LPT)	Experimental (Clift.et.al)	Force balance eq.	Mendelson eq.	Error % with (experimental data)	Error % with (force balance eq.)	Error % with (Mendelson eq.)
2	0.2898	0.3000	0.2877	0.2878	3.40	0.73	0.69
3	0.2533	0.2652	0.2517	0.2518	4.49	0.63	0.59
4	0.2383	0.2509	0.2368	0.2369	5.02	0.63	0.59
5	0.2331	0.2416	0.2317	0.2318	3.52	0.60	0.56
6	0.2332	0.2355	0.2318	0.2319	0.97	0.60	0.56
7	0.2363	0.2386	0.2348	0.2349	0.96	0.64	0.59
8	0.2411	0.2396	0.2397	0.2398	0.63	0.58	0.54
9	0.2471	0.2447	0.2456	0.2457	0.98	0.61	0.57
10	0.2538	0.2447	0.2521	0.2523	3.71	0.67	0.59

at a different case of bubble diameter shown in Table 4. The experimental data were extracted for the case of bubble rising in pure water from [2] using the g3data software.

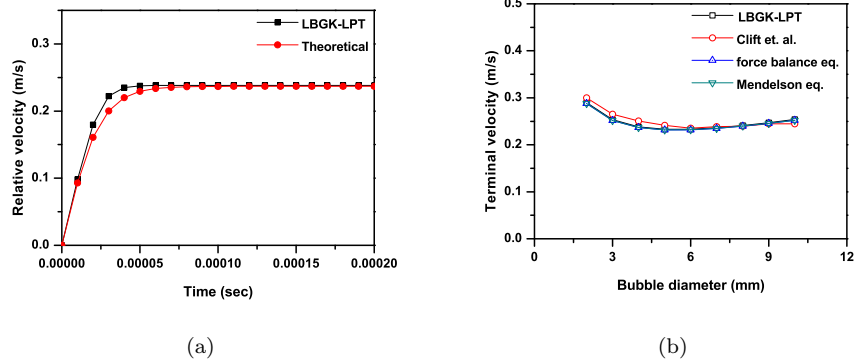


Fig. 2. Comparison of (a) simulated and theoretical relative velocity of 4 mm bubble diameter at different time instant rising in stagnant liquid, (b) simulated, theoretical and experimental terminal velocity at a different case of bubble diameter

Fig.2(a) shows the comparison of simulated and theoretically calculated relative velocity for 4 mm air bubble rising in a quiescent water tank as a function of time. It is seen that after 0.00005 seconds bubble rising with a constant relative velocity. The results obtained from simulation are satisfactory with the theoretical results. Also, it has been observed that bubble takes ≈ 1.86 seconds to reach the top layer of fluid.

Fig.2(b) shows the comparison of simulated terminal velocity from the LBGK-LPT model with the corresponding theoretically and experimentally computed terminal velocity of a bubble motion in a stagnant water tank at varying bubble diameter. It is observed that the simulated results are in good agreement with the theoretical results computed from the eq.(23), (24) and with the experimental results of [2].

Fig.3 shows the velocity fluctuation in continuous liquid phase relative to the motion of air bubble at a different time instant. It is seen that that vortex appeared in the wake region is closer to the edge of a dispersed air bubble.

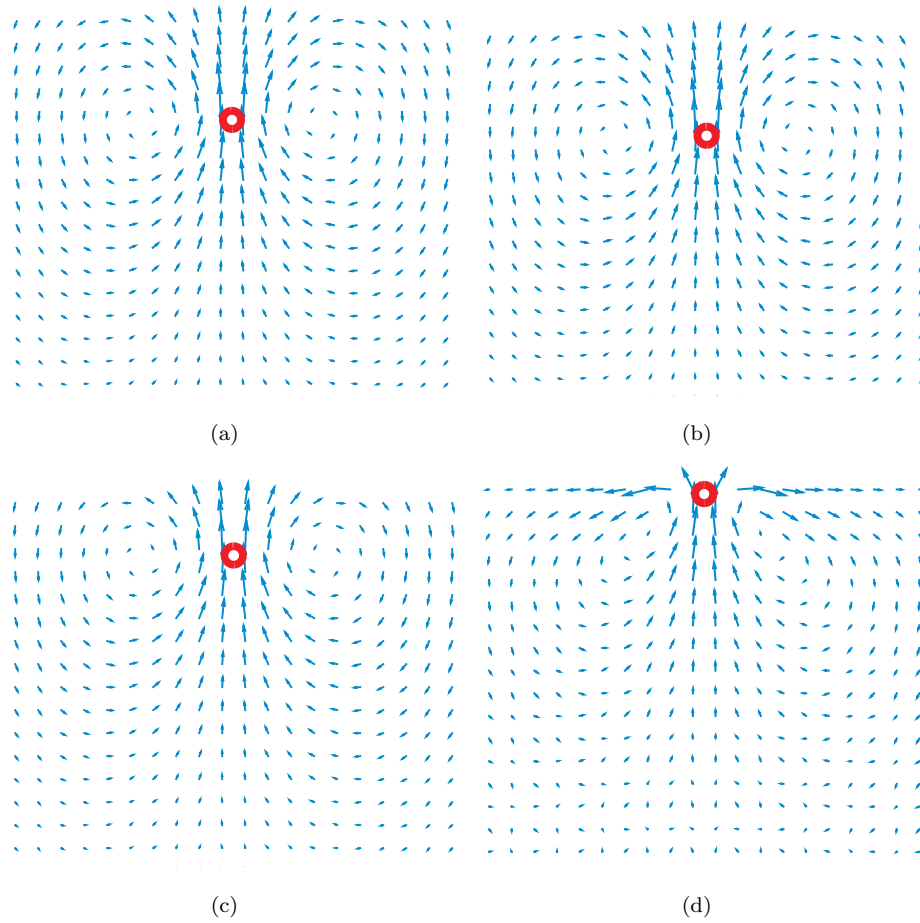


Fig. 3. 2D representation of liquid velocity fluctuation on rising of air bubble at time (a) $t = 0.4632$ sec, (b) $t = 0.9264$ sec, (c) $t = 1.3896$ sec, and (d) $t = 1.85280$ sec

4.2. Grid independence test

As grid size depends on aspect ratio (from eq. (17)), the different aspect ratio was chosen to investigate grid independence test for different cases of bubble diameter. Table 5, shows the grid size at varying aspect ratio for three different cases of bubble diameter (i.e. 4 mm, 8 mm, and 10 mm) and the predicted terminal velocity from simulation for these cases are shown in Table 6.

Table 5: Unit conversion parameters at different range of aspect ratio

Aspect ratio	LCF	MCF	TCF	cell size (Δx)	column width	column depth	water level	bubble diameter	bubble diameter
					in lattice unit	in lattice unit	in column tank	(physical unit)	(lattice unit)
					w_{lu}	d_{lu}	h_{lu}	$d_{b,pu}$ (mm)	$d_{b,lu}$
1.25	200	8000	10000	0.005000	30	30	90	4	0.8
0.625	400	64000	10000	0.002500 = $\Delta x/2$	60	60	180	4	1.6
0.3125	800	512000	10000	0.001250 = $\Delta x/4$	120	120	360	4	3.2
1.25	100	1000	10000	0.010000	15	15	45	8	0.8
0.625	200	8000	10000	0.005000 = $\Delta x/2$	30	30	90	8	1.6
0.3125	400	640000	10000	0.002500 = $\Delta x/4$	60	60	180	8	3.2
1.25	80	512	10000	0.012500	12	12	36	10	0.8
0.625	160	4096	10000	0.006250 = $\Delta x/2$	24	24	72	10	1.6
0.3125	320	32768	10000	0.003125 = $\Delta x/4$	48	48	144	10	3.2

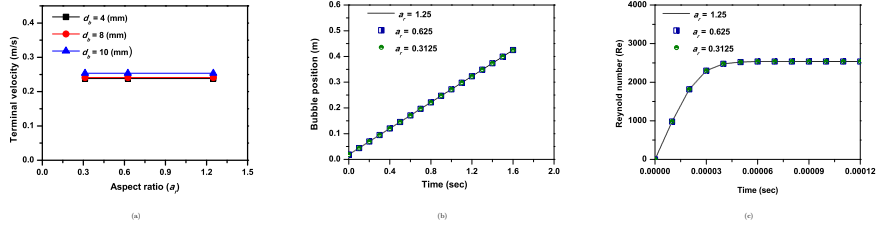


Fig. 4. Grid independence test (a) terminal velocity at varying aspect ratio for three different cases of bubble diameter, (b) bubble position vs time at different aspect ratio for 10 mm bubble diameter, and (c) reynold number (Re) vs time at different aspect ratio for 10 mm bubble diameter

Fig.4(a) shows the terminal velocity of a bubble at varying aspect ratio for three different cases of bubble diameter (i.e. 4 mm, 8 mm and 10 mm). The results within the grid size $30 \times 30 \times 90$ from aspect ratio 1.25 are same as that of the grid size $60 \times 60 \times 180$ and $1200 \times 120 \times 360$ from aspect ratio 0.625 and 0.3125 respectively, for the case of 4 mm bubble diameter. For other two cases of 8 mm and 10 mm bubble diameter, results are also similar for different grid sizes. For the case of 10 mm bubble diameter: the position of the bubble and Reynolds number (Re) on a particular instant of time at different aspect ratio was evaluated and results shown in Fig.4(b) and 4(c) also demonstrate model independence from the grid size.

Table 6: Terminal velocity at varying aspect ratio for three different cases of bubble diameter

Aspect ratio	Grid size	bubble diameter	bubble diameter	Terminal velocity
		(physical unit)	(lattice unit)	
		$d_{b,pu}$ (mm)	$d_{b,lu}$	
1.2500	$30 \times 30 \times 90$	4	0.8	0.2383
0.6250	$60 \times 60 \times 180$	4	1.6	0.2383
0.3125	$120 \times 120 \times 360$	4	3.2	0.2383
1.2500	$15 \times 15 \times 45$	8	0.8	0.2411
0.6250	$30 \times 30 \times 90$	8	1.6	0.2411
0.3125	$60 \times 60 \times 180$	8	3.2	0.2411
1.2500	$12 \times 12 \times 36$	10	0.8	0.2538
0.6250	$24 \times 24 \times 72$	10	1.6	0.2538
0.3125	$48 \times 48 \times 144$	10	3.2	0.2538

4.3. Stability test

The different range of dimensionless relaxation frequency (ω) of LBGK model is applied for investigating the maximum value up to which the solution is stable. For the current study of dispersed gas-liquid flow, the predicted maximum allowed collision frequency for a stable solution is shown in Fig.5. Fig.5 shows the velocity of bubble motion relative to liquid phase velocity as a function of time for a given range of relaxation frequency. As can be seen from Fig.5, the solution goes unstable for a relaxation frequency of 1.98, means the maximum allowed value of relaxation frequency for a stable solution of dispersed gas-liquid flow is 1.97. This depicts that solution becomes unstable for a very low range of liquid phase viscosity (from relation in eq. (9)).

5. Concluding Remarks

A modeling technique to simulate the benchmark problem of dispersed gas-liquid flow (i.e. single bubble rising in a stagnant liquid) using EL approach has

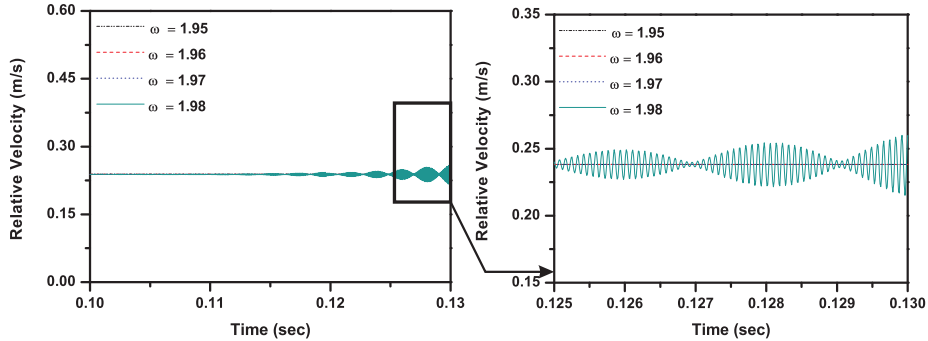


Fig. 5. Numerical stability test for dispersed gas-liquid flow using LBGK-LPT model in the parameter space of bubble relative velocity vs time and at a given value of ω

been presented. The BGK scheme of lattice Boltzmann method (LBM) proposed by [18] was used to discretize the continuous liquid phase. The dispersed gas (air-bubble) phase modeled with the lagrangian particle tracking (LPT) approach. The concept of two-way coupling using cheap-clipped polynomial mapping function given by [9] was used for momentum-transfer between two phases.

We have demonstrated the numerical accuracy of the model by comparing the simulation results for a relative and terminal velocity of the bubble with theoretical and experimental results. The results are in good agreement with the theoretical and available experimental data. Additionally, the velocity fluctuation in the continuous liquid phase due to bubble motion is also presented at a different time instant. The results obtained from the grid independence study shows that model is independent of the grid size. We also performed stability test for the model, and result shows that the model goes unstable for low value of liquid phase viscosity.

Further, the bubble tracking module validated in current work will be used to develop a solver capable of simulating an industrial scale bioreactor with all the complex physical process.

References

References

- [1] X. Frank, D. Funfschilling, N. Midoux, H. Z. Li, Bubbles in a viscous liquid: lattice boltzmann simulation and experimental validation, *Journal of Fluid Mechanics* 546 (2006) 113–122.
- [2] R. Cli, J. Grace, M. Weber, *Bubbles, drops and particles*, Academic Press, 1978.
- [3] S. Sadhal, P. Ayyaswamy, J. Chung, *Transport phenomena with bubbles and drops*, Springer, New York, 1997.
- [4] F. Wenyuan, M. Youguang, J. Shaokun, Y. Ke, L. Huaizhi, An experimental investigation for bubble rising in non-newtonian fluids and empirical correlation of drag coefficient, *Journal of Fluids Engineering* 132 (2) (2010) 021305.
- [5] D. Nie, J. Lin, L. Qiu, X. Zhang, Lattice boltzmann simulation of multiple bubbles motion under gravity, in: *Abstract and Applied Analysis*, Vol. 2015, Hindawi Publishing Corporation, 2015.
- [6] R. Sungkorn, J. Derksen, J. Khinast, Euler–lagrange modeling of a gas–liquid stirred reactor with consideration of bubble breakage and coalescence, *AIChE Journal* 58 (5) (2012) 1356–1370.
- [7] D. Law, F. Battaglia, T. J. Heindel, Numerical simulations of gas-liquid flow dynamics in bubble columns, in: *ASME 2006 International Mechanical Engineering Congress and Exposition*, American Society of Mechanical Engineers, 2006, pp. 593–600.
- [8] R. Sungkorn, J. Derksen, J. Khinast, Modeling of turbulent gas–liquid bubbly flows using stochastic lagrangian model and lattice-boltzmann scheme, *Chemical Engineering Science* 66 (12) (2011) 2745–2757.

- [9] N. G. Deen, M. van Sint Annaland, J. Kuipers, Multi-scale modeling of dispersed gas-liquid two-phase flow, *Chemical Engineering Science* 59 (8) (2004) 1853–1861.
- [10] A. Gupta, Lattice boltzmann simulation to study single and multi bubble dynamics (2007).
- [11] C. K. Aidun, J. R. Clausen, Lattice-boltzmann method for complex flows, *Annual review of fluid mechanics* 42 (2010) 439–472.
- [12] S. Chen, G. D. Doolen, Lattice boltzmann method for fluid flows, *Annual review of fluid mechanics* 30 (1) (1998) 329–364.
- [13] H. Huang, J.-J. Huang, X.-Y. Lu, A mass-conserving axisymmetric multi-phase lattice boltzmann method and its application in simulation of bubble rising, *Journal of Computational Physics* 269 (2014) 386–402.
- [14] S. Succi, *The lattice Boltzmann equation: for fluid dynamics and beyond*, Oxford university press, 2001.
- [15] D. Darmana, N. G. Deen, J. Kuipers, Parallelization of an euler-lagrange model using mixed domain decomposition and a mirror domain technique: Application to dispersed gas-liquid two-phase flow, *Journal of Computational Physics* 220 (1) (2006) 216–248.
- [16] E. Delnoij, F. Lammers, J. Kuipers, W. P. M. van Swaaij, Dynamic simulation of dispersed gas-liquid two-phase flow using a discrete bubble model, *Chemical engineering science* 52 (9) (1997) 1429–1458.
- [17] S. K. Kang, Y. A. Hassan, A comparative study of direct-forcing immersed boundary-lattice boltzmann methods for stationary complex boundaries, *International Journal for Numerical Methods in Fluids* 66 (9) (2011) 1132–1158.
- [18] P. L. Bhatnagar, E. P. Gross, M. Krook, A model for collision processes in gases. i. small amplitude processes in charged and neutral one-component systems, *Physical review* 94 (3) (1954) 511.

- [19] D. A. Perumal, A. K. Dass, A review on the development of lattice boltzmann computation of macro fluid flows and heat transfer, *Alexandria Engineering Journal* 54 (4) (2015) 955–971.
- [20] R. Zhang, H. Chen, Lattice boltzmann method for simulations of liquid-vapor thermal flows, *Physical Review E* 67 (6) (2003) 066711.
- [21] X. He, L.-S. Luo, Lattice boltzmann model for the incompressible navier-stokes equation, *Journal of statistical Physics* 88 (3) (1997) 927–944.
- [22] X. He, Q. Zou, L.-S. Luo, M. Dembo, Analytic solutions of simple flows and analysis of nonslip boundary conditions for the lattice boltzmann bgk model, *Journal of Statistical Physics* 87 (1) (1997) 115–136.
- [23] Z. Guo, C. Zheng, B. Shi, Discrete lattice effects on the forcing term in the lattice boltzmann method, *Physical Review E* 65 (4) (2002) 046308.
- [24] B. Ničeno, M. Boucker, B. Smith, Euler-euler large eddy simulation of a square cross-sectional bubble column using the neptune_cfd code, *Science and Technology of Nuclear Installations* 2009.
- [25] A. Kitagawa, Y. Murai, F. Yamamoto, Two-way coupling of eulerian-lagrangian model for dispersed multiphase flows using filtering functions, *International journal of multiphase flow* 27 (12) (2001) 2129–2153.
- [26] Q. Zou, X. He, On pressure and velocity boundary conditions for the lattice boltzmann bgk model, *Physics of fluids* 9 (6) (1997) 1591–1598.
- [27] H. D. Mendelson, The prediction of bubble terminal velocities from wave theory, *AIChE Journal* 13 (2) (1967) 250–253.
- [28] R. Krishna, M. Urseanu, J. Van Baten, J. Ellenberger, Wall effects on the rise of single gas bubbles in liquids, *International communications in heat and mass transfer* 26 (6) (1999) 781–790.

Appendix A. Physical to lattice unit conversion

The simulation of continuous liquid phase through lattice Boltzmann method (LBM) requires the conversion of physical unit to lattice unit. This can be performed as:

$$C.F. = lu/pu \quad (A.1)$$

where $C.F.$ is the conversion factor for the conversion of physical unit (pu) to lattice unit (lu). With the reference of eq. (A.1), the corresponding length ($L.C.F.$), time ($T.C.F.$) and mass ($M.C.F.$) conversion factor can be defined as:

$$L.C.F. = l_{lu}/l_{pu}, \quad T.C.F. = t_{lu}/t_{pu}, \quad M.C.F. = m_{lu}/m_{pu} \quad (A.2)$$

From the geometrical parameters, we have

$$h_{pu} = 0.45 \text{ mm}, w_{pu} = 0.15 \text{ mm}, d_{pu} = 0.15 \text{ mm} \quad (A.3)$$

where h_{pu} , w_{pu} and d_{pu} be the level of water in rectangular column tank, width and depth column tank in physical unit respectively. According to [24], the aspect ratio (i.e. the ratio between the grid spacing of continuous liquid domain to bubble diameter) was chosen to be 1.25. Thus,

$$\Delta x_{pu}/d_{b,pu} = 1.25 \quad (A.4)$$

where Δx_{pu} and d_b represents the grid spacing and bubble diameter respectively. Solving eq. (A.4) for the case of 4 mm bubble diameter, we can obtain:

$$\Delta x_{pu} = 0.005 \quad (A.5)$$

From eq. (B.2), we have:

$$L.C.F. = \Delta x_{lu}/\Delta x_{pu} \quad (A.6)$$

For the lattice boltzmann method, the lattice size (Δx_{lu}) and the time step size (Δt_{lu}) are

$$\Delta x_{lu} = \Delta t_{lu} = 1 \quad (A.7)$$

Thus, using the value of Δx_{pu} from eq. (A.5), value of $L.C.F$ can be easily evaluated from eq. (A.7) gives:

$$L.C.F. = 200 \tag{A.8}$$

From eq. (A.2), (A.3), and (A.8) we have

$$h_{lu} = 90, w_{lu} = 30, d_{lu} = 30, d_{b,lu} = 0.8 \tag{A.9}$$

Where h_{lu} is level of water in column tank, w_{lu} is width of column tank and $d_{b,lu}$ is the diameter of bubble in lattice unit. The liquid time step has taken to be 0.0001 sec in the physical unit for the simulation i.e. Δt_{pu} . Thus, we compute the $T.C.F$ using the relation from eq. (A.2) we have

$$T.C.F = \Delta t_{lu} / \Delta t_{pu} = 1 / 0.0001 = 10000 \tag{A.10}$$

The density of continuous (liquid) phase in the lattice unit ρ_{lu} and physical unit ρ_{pu} are taken to be:

$$\rho_{lu} = 1, \rho_{pu} = 1000 \tag{A.11}$$

Correspondingly, the $M.C.F$ can be calculated by the given relation:

$$\rho_{pu} = \rho_{lu} (LCF^3 / MCF) \tag{A.12}$$

which gives,

$$M.C.F = 8000 \tag{A.13}$$

List of Figures

1	Schematic representaion of D_3Q_{19} lattice structure	5
2	Comparison of (a) simulated and theoretical relative velocity of 4 mm bubble diameter at different time instant rising in stagnant liquid, (b) simulated, theoretical and experimental teriminal velocity at a different case of bubble diameter	13
3	2D representation of liquid velocity fluctuation on rising of air bubble at time (a) $t = 0.4632$ sec, (b) $t = 0.9264$ sec, (c) $t = 1.3896$ sec, and (d) $t = 1.85280$ sec	14

4	Grid independence test (a) terminal velocity at varying aspect ratio for three different cases of bubble diameter, (b) bubble position vs time at different aspect ratio for 10 mm bubble diameter, and (c) reynold number (Re) vs time at different aspect ratio for 10 mm bubble diameter	15
5	Numerical stability test for dispersed gas-liquid flow using LBGK-LPT model in the parameter space of bubble relative velocity vs time and at a given value of ω	17